UDC 62-932.4

Y. Ivanchuk[1], PhD, Assoc. Prof.
Vinnytsia National Technical University, 95 Khmelnitske Shosse, Vinnytsia, Ukraine, 21021; e-mail: ivanchuck@ukr.net

MATHEMATICAL MODELING OF THE TECHNOLOGICAL PROCESS OF THE ROCK DESTRUCTION BY A VIBRO IMPACT DEVICE WITH A HYDRO PULSE DRIVE

Я.В. Іванчук. **Математичне моделювання технологічного процесу руйнування гірської породи віброударним пристроєм з гідроімпульсним приводом.** Доведено високу ефективність технологічного процесу руйнування гірської породи за допомогою віброударних навантажень. Високий ступінь інтенсифікації процесу руйнування гірської породи досягається застосуванням розробленої оригінальної конструкції віброударного пристрою з гідроімпульсним приводом на базі двокаскадного клапана–пульсатора. Розроблено нову математичну модель для дослідження технологічних процесів руйнування гірської породи віброударним пристроєм на базі законів гідродинаміки із використанням узагальнених законів механіки. При розробці математичної моделі технологічний процес було досліджено над двух фазах: фаза накопичення кінетичної енергії, а також фаза ударної взаємодії робочого органу віброударного пристрою із поверхнею гірської породи. Математична модель ударної взаємодії була побудована на основі моделі удару Сірса а системи рівнянь напружено–деформованого стану. На основі розробленої математичної моделі методом кінцевих об'ємів за допомогою чисельного моделювання отримано розподіл тиску і швидкості робочої рідини в гідроімпульсному приводі віброударного пристрою. За допомогою чисельного методу кінцевих елементів отримано розподіл напружень у робочому органі і елементу гірської породи при віброударному руйнуванні. Аналіз розрахунку власних частот робочого органу показав стійку роботу віброударного пристрою у дорезонансних режимах. Отримані робочі залежності основних робочих характеристик віброударного пристрою на базі гідроімпульсного приводу дозволили розробити рекомендації для подальшого підвищення ефективності технологічного процесу. Отримані результати чисельного моделювання технологічних процесів руйнування гірської породи віброударним пристроєм на базі гідроімпульсного приводу, показали перевагу обраного підходу до проектування, а також дозволив довести ефективність розробленої конструкції.
Ключові слова: імпульс, гірська порода, удар, вібрації, математична модель, гідропривод, клапан

Y. Ivanchuk. **Mathematical modeling of the technological process of the rock destruction by a vibro impact device with a hydro pulse drive.** The high efficiency of the technological process of destruction of the rock with the help of vibration of shock loads has been proved. A high degree of intensification of the process of rock destruction is achieved by using the developed original design of a vibro–impact device with a hydro-pulse drive based on the two–stage pulsate valve. A new mathematical model has been developed for studying of technological processes of rock destruction using a vibro–impact device based on the laws of hydrodynamics using the generalized laws of mechanics. When developing a mathematical model, the technological process was investigated over two phases. This is the phase of kinetic energy accumulation, as well as the phase of the impact interaction of the working body of the vibro–impact device with the surface of the rock. The mathematical model of the shock interaction was built based on the Sears impact model and the system of equations of the stress–strain state. Based on the developed mathematical model and using the finite volume method as well as the numerical simulation, the pressure and velocity of the working fluid in a hydro–pulse drive of a vibro–impact device are obtained. Using the numerical finite element method, the stress distribution in the working body of the vibro–impact device and the rock element during vibro-impact destruction is obtained. Analysis of the calculation of the natural frequencies of the working body showed the stable operation of the vibro-impact device in the preresonance modes. The obtained working dependences of the main performance characteristics of the vibro-impact device based on the impulse allowed us to develop recommendations for further improving the efficiency of the technological process. The obtained results of numerical simulation of rock destruction technological processes by a vibro impact device based on a hydro–impulse reason, showed the advantages of the chosen design approach, and allowed to prove the effectiveness of the developed design.
Keywords: impulse, rock formation, shock, vibrations, mathematical model, hydraulic drive, valve

Introduction. Increasing the effectiveness of social production based on its comprehensive intensification and further acceleration of scientific and technological progress, involves the creation and introduction into the production of new technology and advanced technology. In the mining industries to equipment that meets the task, include impact machines. They allow significantly increasing the efficiency of secondary crushing of rocks in open mining operations and the development of frozen soils in quarries and in construction [1]. The use of shock machines for the destruction of rocks opened the way where significant productivity is achieved not by increasing the power of base machines, but by increasing the energy of single strikes, increasing the frequency of strokes when fully utilizing the power of base machines. However, the experience of using shock impact machines has led to the solu-

DOI: 10.15276/opu.2.55.2018.01

ISSN 2076-2429 (print)
ISSN 2223-3814 (online)

tion of a number of problems, the understanding of which is impossible without analyzing the impact of shock impulses on a destructive environment. It is also impossible without analyzing the dynamics of the hinged equipment of the entire machine under the influence of loads from the working shock mechanism [2].

Analysis of literary data and problem statement. In the article [3] systems with multi-mode shock–vibration units are considered. They represent dynamic systems with nonlinear performance, in which vibration is combined with blows. The work of such shock-vibration units is carried out in the mode of nonlinear oscillations of the working body. This paper defines the optimal relationships between the period of the excitatory force and the period of forced oscillations in a shock–vibration system.

The work of the vibration units, which are considered in the article [4], is based on the nonlinearity of characteristics of the elasticity of the medium with the material being processed and the change of characteristics depending on the time. As a result, the dynamic characteristics of the installation are improved and the operation of the installation is possible in modes using higher harmonic components of the vibration of the working body. In such modes, the energy consumption of a vibration unit is significantly reduced.

In the article [5] the results of analysis of modes of harmonic oscillations are given. In the article [5] a mathematical model of the system "vibration installation – concrete mix" with discrete parameters of a concrete mixture as a medium is considered. Such a mathematical model has certain limitations. As shown in [5], with a certain correlation between the oscillation period and the time period required to pass the wave of oscillations in the medium, the mathematical model with discrete environmental parameters becomes false.

Therefore, the construction of a mathematical model that will allow investigating the technological process of rock destruction during a pulse loading at different operating modes of a hydropulse drive of a vibro impact device in order to determine the basic performance characteristics is an urgent task.

Purpose and tasks of the research. The aim of the work is to increase the efficiency of the theoretical study of the technological process of crushing the rock through the development of perspective mathematical models of physical processes of impulse destruction by vibro impact devices based on the hydropulse drive (HPD).

To achieve this goal, the following tasks were solved:

– to develop an effective structure of a vibro impact device with a HPD, based on a two-stage valve-pulsator, to implement the most effective modes of impulse influence on the treated environment;

– to develop a mathematical model of the technology of rock crushing by a vibro–impact device based on the HPD with a two-stage valve–pulsator;

– on the basis of the developed mathematical model to obtain working dependences for determining the basic performance characteristics of the technological process.

Materials and methods of research. In the Vinnytsia National Technical University, the department of industry mechanical engineering for the effective destruction of rocks based on GIP with a two–stage valve with a pulsator [6, 7]. Fig. 1 shows a three–dimensional CAD–model of a hinged vibro–impact device based on HPD.

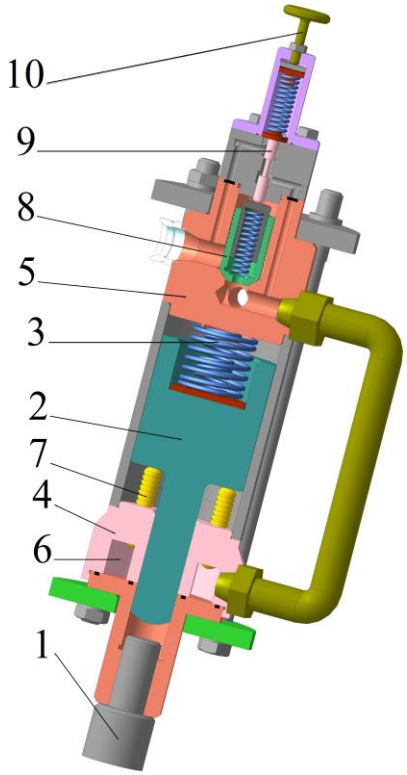

Fig. 1. Three-dimensional model of hinged vibro-impact device on the basis of HPD

Attached vibro impact device consists of a working body 1 (a bit with a conical tip). On its upper base, a periodic impact load is applied to the impact mass 2 under the action of gravity forces and the forces of return of the elastic element 3.

The reciprocating motion of the shock mass 2 occurs due to the action of the hydropulse drive, which consists of a hydraulic cylinder 4 and a pulse generator of pressure 5 (two–stage pulsating valve). In the working cavity (see Fig. 1), the hydraulic cylinder 4 creates a periodic pressure change with the amplitude $\Delta p=p_1–p_2$, which is transmitted to the hydraulic cylinder 7.

In turn, the plunger, under the action of the current pressure in the cavity 6 of the hydraulic cylinder 4, moves the impact mass 2, which causes deformation of the elastic element 3 and the accumulation of potential energy from the forces of gravity.

After the valve of the second cascade 8 opening there is a drain of the working fluid, which causes the pressure drop in the working cavity of the hydraulic cylinder 4. In this case, the shock mass 2 moves to its original position, which causes a shock interaction with the working body 1.

The energy of the shock interaction consists of the potential energy of the return forces of the elastic element 3 and the forces of gravity of the impact mass 2. The adjustment of the pressure of the pressure p_2 of the pulse pressure generator 5 depends on the adjustment of the spring 10, and the regulation of the connection of the pressure line with the drain valve of the second cascade 8 (resetting of the working pressure to pressure p_1) occurs with the help of the locking element 9 (valve of the first cascade) in the form of a spool.

Fig. 2 presents a three–component (flat, multivariate) inertial model with non–constricted contacts between the masses, which allows to simulate elastoplastic deformations of rock 7 by x, y, z.

ISSN 2076-2429 (print)
ISSN 2223-3814 (online)

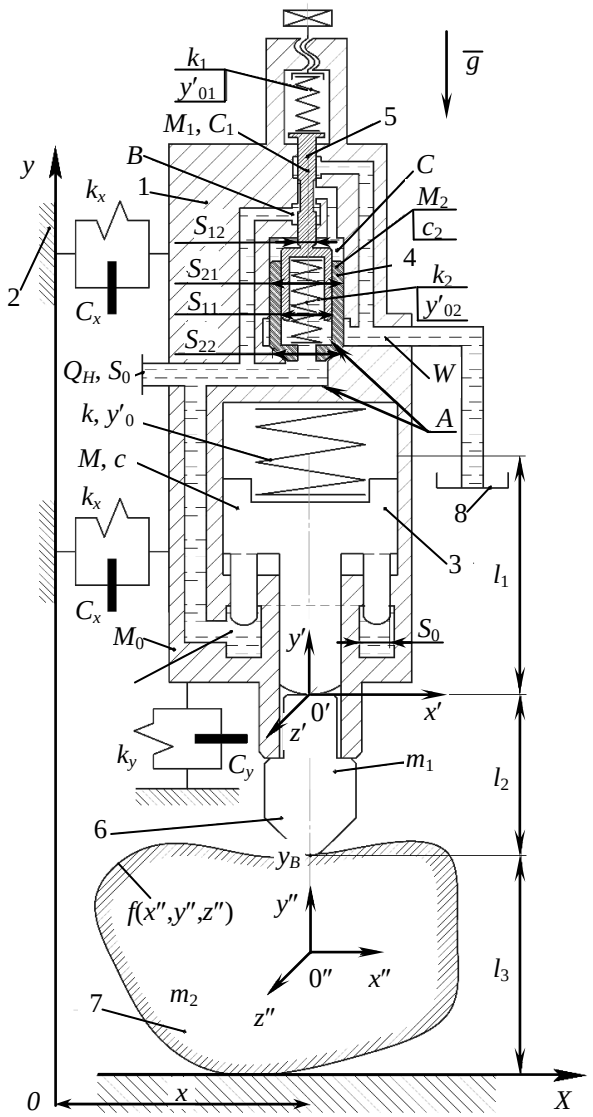

Fig. 2. Dynamic model of the technological process of destruction of the rock by a hinged vibro-impact device from the HPD on the basis of an elastic-plastic strain-strain solid-state model

We introduce the motion of the coordinate system $x'0'y'z'$, rigidly connected with the body 1 of the vibro impact device of mass M_0, and the fixed coordinate system $x''0''y''z''$, rigidly connected to the main central axes of inertia of the rock 7 , whose surface is represented by a three-dimensional surface function. We also introduce an absolute (stationary) $x0y$ coordinate system.

The mathematical model of the technological process of rock formation destruction by a hydropulse vibro impact device should be considered as one consisting of two periods: the period of accumulation of kinetic energy and the period of shock interaction.

The period of accumulation of kinetic energy of the technological process of the destruction of the rock by a hydropulse vibro impact device consists of the characteristic working movements of the stop elements 4, 5 and the inertial mass 3.

In turn, the period of shock interaction is characterized by elastic–plastic deformations of inertial mass 3, shock mass 6 and rock 7 in the places of their contact interaction.

Consider a longer working period of accumulation of kinetic energy. Let's record the equation of motion for body 1 of a vibro impact device of mass M_0:

$$\begin{cases} -M_0\ddot{y} = -M_0 g + k_1(y'_{01} + y'_1) + k(y'_0 + y') - \iint\limits_{\tilde{S}} p_{\tilde{S}}(t)dS_y + c_y\dot{y} + c_1\dot{y}'_1 + c_2\dot{y}'_2 + c\dot{y}' + k_y y - N_{04y} + N_{06y}; \\ -M_0\ddot{x} = -\iint\limits_{\tilde{S}} p_{\tilde{S}}(t)dS_x + 2c_x\dot{x} + 2k_x x - N_{06x}, \end{cases} \quad (1)$$

where $p_{\tilde{S}}(t)$ – function of pressure change of the working fluid in the internal hydraulic channels of the vibro impact device 1;

$\iint\limits_{\tilde{S}} p_{\tilde{S}}(t)dS_y$, $\iint\limits_{\tilde{S}} p_{\tilde{S}}(t)dS_x$ – corresponding components of forces acting on the inner surface of the cavity of the hydraulic channels of the vibro impact device 1;

c_1 – coefficient of viscous friction forces between the walls of the body of the vibration shock device 1 and the valve of the first cascade 5;

c_2 – coefficient of viscous frictional forces between the walls of the body of the vibro impact device 1 and the valve of the second cascade 4;

c – coefficient of viscous friction forces between the walls of the body of the vibro impact device 1 and the inertial mass 3;

c_y, c_x – vertical and horizontal components of the coefficient of viscous friction of the damping component of the damping unit, which connects the hydropulse vibro impact device with the boom of the vehicle [8];

N_{04y} – Vertical components of the reaction forces of the conical valve of the second cascade 4 to the conic resistance of the body of the vibro impact device 1;

N_{06x}, N_{06y} – horizontal and vertical components of the forces of reaction of shock mass 6 on the surface of the body of the vibration shock device 1;

k_1 – stiffness of the valve spring of the first cascade 5;

k – torsional spring of inertia mass 3;

k_y, k_x – vertical and horizontal components of the stiffness of the elastic component of the shock absorber, which connects the hydropulse vibro impact device 1 with the boom of the vehicle [8];

y'_{01} – preliminary tension of the spring of the valve of the first cascade;

y'_0 – preliminary tension of the spring of the inertial mass.

Equation of motion for an inertial mass 3 weighed by Mg

$$M\ddot{y}_3 = -Mg - k(y'_0 + y') + \iint\limits_{3S_0} p_{S_0}(t)dS - c(\dot{y}_3 - \dot{y}'_3) + N_{36_y}, \quad (2)$$

where $p_{S_0}(t)$ – function of pressure change of the working fluid in the internal pressure cavity D two-stage valve-pulsator;

$\iint\limits_{3S_0} p_{S_0}(t)dS$ – the corresponding components of the forces acting on the lower surface S_0 of the plungers of the inertial mass 3;

N_{36y} – the vertical component of the force of the reaction of the impact mass 6 on the inertial mass 3.

Equation of motion for the valve of the first cascade 5 weighing $M_1 g$:

$$M_1\ddot{y}_1 = -M_1 g - k_1(y'_{01} + y') + k_2(y'_{02} + y'_1 - y'_2) + \iint\limits_{S_{12}} p_{S_{12}}(t)dS - c_1\dot{y}'_1 - c_1(\dot{y}'_1 - \dot{y}_1), \quad (3)$$

where $p_{S_{12}}(t)$ – function of pressure change of a working fluid in internal pressure A, C, B and drain W cavities of a two-stage valve–pulsator;

$\iint\limits_{S_{12}} p_{S_{12}}(t)dS$ – corresponding force components acting on the bottom surface S_{12} of the valve of the first cascade 5;

ISSN 2076-2429 (print)
ISSN 2223-3814 (online)

k_2 – stiffness of the spring of the valve of the second cascade 4;

y'_{02} – previous tension of valve spring of the second cascade 4.

Equation of motion for the valve of the second cascade 4 M_2g weight:

$$M_2\ddot{y}_2 = -M_2g - k_2(y'_{02} + y'_1 - y'_2) + \iint\limits_{(S_{21}-S_{22})} p_{(S_{21}-S_{22})}(t)dS + c_1(\dot{y}' - \dot{y}'_1) - c_2\dot{y}'_2 + N_{40_y}, \quad (4)$$

where $p_{S_{12}}(t)$ – function of pressure change of a working fluid in internal pressure *A*, *C*, *B* and drain *W* cavities of a two-stage valve-pulsator;

$\iint\limits_{(S_{21}-S_{22})} p_{(S_{21}-S_{22})}(t)dS$ – corresponding components of the forces acting on the lower surface $S_{21} - S_{22}$ of the valve of the second cascade 4;

N_{40y} – vertical components of the reaction forces of the conical support of the body of the vibro impact device 1 to the valve of the second cascade 4.

The law of motion for a shock mass 6 weighing m_1g:

$$\begin{cases} m_1\ddot{y}_{11} = -m_1g - N_{60y} + N_{67y} - N_{63y}; \\ m_1\ddot{x}_{11} = N_{60x}, \end{cases} \quad (5)$$

where N_{60x}, N_{60y} – horizontal and vertical components of the reaction forces of the body of the vibro impact device 1 on the surface of the impact mass 6;

N_{67y} – the force of the reaction of rock 7 to the impact mass 6;

N_{63y} – vertical component of the reaction force of the inertial mass 3 on the impact mass 6.

In this case, we also neglected the inertial forces of the working fluid acting on the working bodies of the hydropulse vibro impact device, as having a small contribution to the movement of the device as a whole.

In order to completely record the mathematical model of the operation of the hydropulse vibro impact device, we need to consider the operation of the HPD at the appropriate working phases of the two-stage valve-pulsator.

1) Pressure set phase. In this phase, the conical valve of the second cascade 4 of mass M_2 and the spool valve of the 5th mass M_1 are in a state of rest. In this phase, the conical valve of the second cascade 4 overlaps the pressure cavities *A*, *B*, *D* from the drainage cavity *W* (see Fig. 2), and the spool one-stage valve 5 overlaps the pressure cavities *B* and *C* from the drainage cavity *W*, which causes a set of pressure in the pressure cavities *A* and *D*, therefore the main pressure pressure acts on the area S_0 of the lower base of the inertial mass 3.

It should be noted that this phase occurs during the time t when the impact mass 6 is in contact with the surface of the rock 7. The coordinate of the contact point of the impact mass 6 and the rock 7 – (*x*, l_3, 0). In this phase, the inertia mass 3 is moving.

For this phase $0 \le t \le t_{ps}$ we write the following initial conditions:

$$\begin{cases} \iint\limits_{S_{12}} p_{S_{12}}(t)dS \le k_1y'_{01}; \quad \iint\limits_{(S_{21}-S_{22})} p_{(S_{21}-S_{22})}(t)dS \le k_2y'_{02}; \\ \dot{y}'_1(t) = \dot{y}'_2(t) = 0; \quad 0 \ge y'(t) \ge y'_{\max}; \quad N_{63y} = N_{36y} = 0. \end{cases} \quad (6)$$

where $y'_{\max}$ – maximum strok of inertia mass *M*.

2) The phase of operation (opening) of a two-stage valve-pulsator. In this phase, the pressure $\iint\limits_{S_{12}} p_{S_{12}}(t)dS$ from the pressure $p_{S_{12}}(t)$ acting on the area S_{12} of the valve of the first cascade 5 is equal to the force of adjusting the regulating spring $k_1y'_{01}$, that is $\iint\limits_{S_{12}} p_{S_{12}}(t)dS \ge k_1y'_{01}$, causing its opening.

When opening the valve of the first cascade 5 there is a combination of pressure cavities *B* and *C* with drainage cavity *W*. This combination of cavities causes a drop in pressure in the pressure cavity *C*, which in turn causes a pressure drop in the pressure cavities *A* and *C*. The result of the pressure difference in pressure cavities *A* and *C* is the emergence of a driving force that forces the valve of the second cascade 4 to move. In this case, the opening of the valve of the second cascade 4 and, respectively, the combination of the pressure cavity *A* and the drainage cavity *W*.

In this phase, there is also the movement of the inertia mass *M* to the maximum displacement $y'_{\max}$, the valve of the first cascade M_1 to the value of maximum opening $y'_{1\max}$ and the valve of the second cascade M_2 to the magnitude of the maximum opening $y'_{2\max}$. Therefore, for this phase $t_{ps} \le t \le t_{op}$ we write the following initial conditions:

$$\begin{cases} \iint\limits_{S_{12}} p_{S_{12}}(t)dS \ge k_1 y'_{01}; \quad \iint\limits_{(S_{21}-S_{22})} p_{(S_{21}-S_{22})}(t)dS \ge k_2 y'_{02}; \quad N_{40y} = N_{04y} = 0; \; N_{63y} = N_{36y} = 0; \\ 0 \ge y'(t) \ge y'_{\max}; \; 0 \ge y'_1(t) \ge y'_{1\max}; \; 0 \ge y'_2(t) \ge y'_{2\max}; \; N_{40x} = N_{04x} = 0, \end{cases} \tag{7}$$

3) The closing (lowering) phase of the two-stage valve-pulsator. In this phase, a working fluid drain occurs due to the drainage cavity *W* in the water jack 8 causing the pressure drop in the pressure cavities *A, B, C, D*. In this case, the valve of the first cascade 5 begins to fall to its original position (the place of the overlapping of the pressure cavities *B* and *C* with drainage cavity *W*). After the pressure cavities *B* and *C* have been detached from the discharge cavity *W*, the pressure in the pressure cavities *B* and *C* sharply begins to increase, in comparison with the pressure in the middle of the valve of the second cascade 4, the pressure cavity *A*. As a consequence of the pressure difference in the pressure cavities *B, C* and *A* are the driving hydraulic force [9], which, together with the force of the spring tension of the valve of the second cascade 4, $k_2(y'_{02} + y'_2)$ causes the valve itself of the second cascade 4 to return to its original position. In this case there is an overlapping of pressure cavities *A* and *D* from the drainage cavity *W*.

In this phase, the reverse movements of the inertia mass *M*, the valve of the first cascade M_1 and the valve of the second cascade M_2 to the initial position also occur. Therefore, for this phase $t_{op} \le t \le t_{cl}$ we write the following initial conditions:

$$\begin{cases} \iint\limits_{S_{12}} p_{S_{12}}(t)dS \ge k_1 y'_{01}; \quad \iint\limits_{(S_{21}-S_{22})} p_{(S_{21}-S_{22})}(t)dS \ge k_2 y'_{02}; \; N_{40y} = N_{04y} = 0; \; N_{63y} = N_{36y} = 0; \\ 0 \ge y'(t) \ge y'_{\max}; \; 0 \ge y'_1(t) \ge y'_{1\max}; \; 0 \ge y'_2(t) \ge y'_{2\max}; \; N_{40x} = N_{04x} = 0. \end{cases} \tag{8}$$

Consider the period of shock interaction of the inertial mass 3, the shock mass 6, and also the rock 7. For this period, the following general initial conditions for the equations of the body of the body $1 - N_{06y} = 0$. The generalizing forces acting on the shock mass 3 from equation (1) are representable, like $\sum F_3 = ky'_0 + cV_0$ and $\sum F_{p_3} = -3p_0 S_0$ where V_0 is the velocity of the shock mass 3 at the end of the closure (lowering) phase of the two-stage valve-pulsator.

The beginning of the absolute fixed axis of the coordinates *OY* will be placed at the upper point of the inertial mass 3 and directed vertically downwards. Similarly, fasting with a fixed system of coordinates $x''0''y''z''$, which is rigidly connected with the main central axes of inertia of rock 7.

The inertial mass 3 and the shock mass 6 are represented in the form of cylindrical stepped rods $00'_1$, $0'_1X_A$, $X_A0'_2$, $0'_2X_C$ and the conic rod X_CX_B,, and the shock surfaces of which are represented as flat round surfaces (Fig. 3).

ISSN 2076-2429 (print)
ISSN 2223-3814 (online)

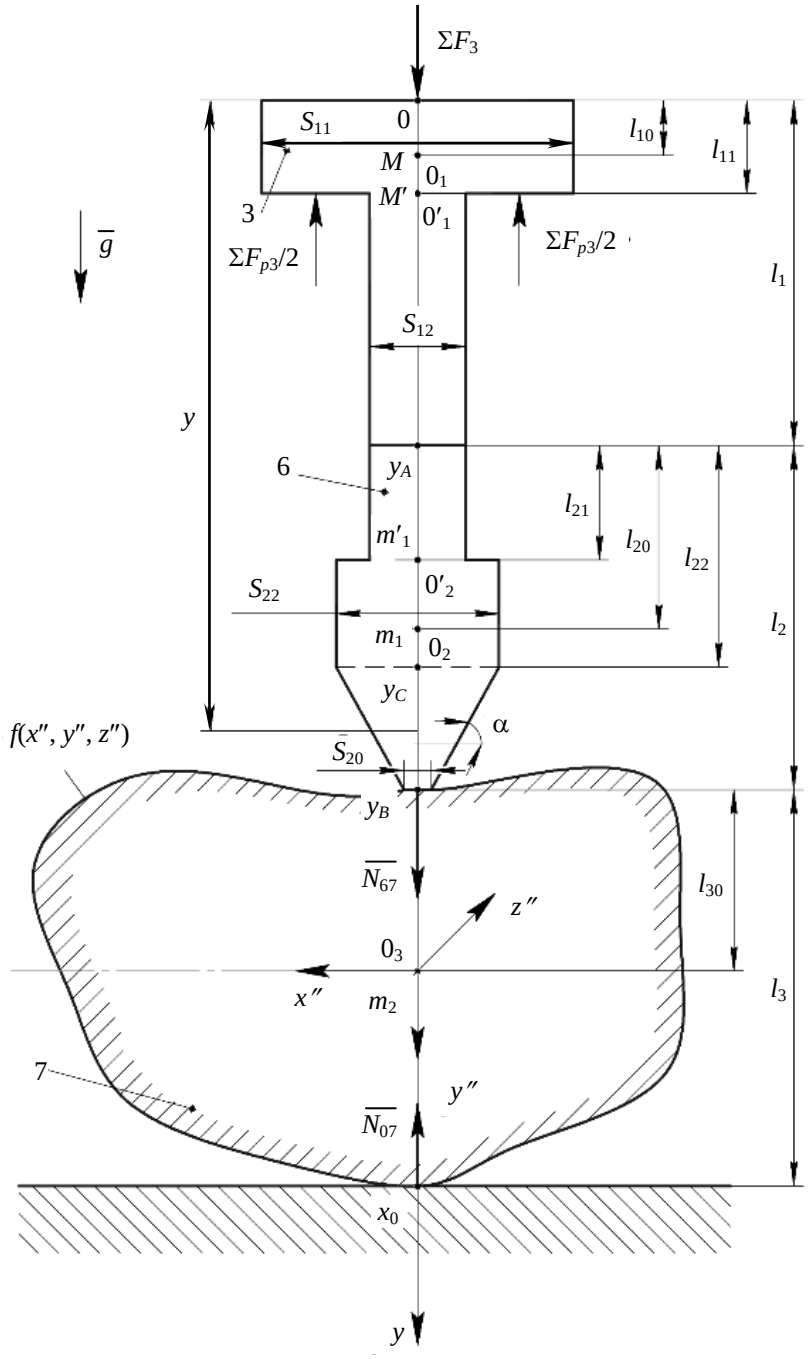

Fig. 3. Dynamic model of impact interaction of inertial 3 and shock 6 masses, as well as rock 7 on the basis of the model of Cirs and elastoplastic model of solids

Each elementary cylindrical rod is expressed by geometric parameters such as:

1. The length l_{11} and the cross-sectional area S_{11} for the rod $00'_1$.
2. The length (l_1–l_{11}) and the cross-sectional area S_{12} for the rod $0'_1X_A$.
3. The length of l_{21} and the cross-sectional area S_{12} for the rod $X_A0'_2$.
4. The length (l_{22}–l_{21}) and the cross-sectional area S_{22} for the rod $0'_2X_C$.

The centers of the masses of the inertial mass 3, the impact mass 6 and the rock 7 are at the corresponding points 0_1, 0_2, 0_3. Let's give the center of gravity of the inertial mass 3 to the point $0'_1$, which

is on the verge of the two cylindrical rods $0'_1$ and $0'_1X_A$. To do this, from the condition of equilibrium of the moments of the force of weight relative to the point 0 [10], we write: $M'=M(l_{10}/l_{11})$.

In the same way, we give the center of gravity of the shock mass 6 to the point $0'_2$, which is on the verge of the two cylindrical rods $X_A0'_2$ i $0'_2X_C$. To do this, from the equilibrium condition of the moments of the force of weight relative to the point X_A [4, 8], we write: $m'_1=m_1(l_{21}/l_{20})$.

To simulate the shock interaction of the inertial mass 3, the shock mass 6, and also the rock 7, we use the Sears model [11], which combines the Hertz approach [6], which takes into account only the local deformation of co-inflicted bodies, and the Saint–Venant's approach [8], which takes into account the general dynamic deformation of bodies when struck.

The motion of the inertial mass 3, the impact mass 6, as well as the rock 7 occurs along the y axis, the beginning of which we place at the point O.

The motion of the cross sections of the rods $00'_1$, $0'_1X_A$, $X_A0'_2$, $0'_2X_C$, X_CX_B is described by the wave equations (10) and the initial conditions (11), which determine the state of the rods $00'_1$, $0'_1X_A$, $X_A0'_2$, $0'_2X_C$, X_CX_B absolutely solids at $t=t_0=0$.

In the system of equations (9) $a_1=\sqrt{E_1/\rho_1}$, $a_2=\sqrt{E_2/\rho_2}$ – the propagation velocity of the elastic wave in the material of the inertial mass 3 and the impact mass 6, respectively; E_1, E_2 – modulus of elasticity of materials of inertial mass 3 and shock mass, respectively, 6; ρ_1, ρ_2 – the density of the materials of the inertial mass 3 and the impact mass, respectively, 6;

$S(y)=S_{22}-(S_{22}-S_0)\left(\frac{y-l_1-l_{22}}{l_2-l_{22}}\right)$ – the cross-sectional area of the rod X_CX_B, whose position is determined by the coordinate y (see Fig. 2); $u_1(y, t)$, $u_2(y, t)$, $u_3(y, t)$, $u_4(y, t)$, $u_5(y, t)$ – longitudinal displacement of the cross sections of the roots of the rods $00'_1$, $0'_1X_A$, $X_A0'_2$, $0'_2X_C$, X_CX_B respectively. In the system of equations (10), $y_{m_1}(0)=l_1+l_{21}$, $y_{M'}(0)=l_{11}$ – the coordinates of absolutely solid bodies at the initial moment of time; $\dot{y}_{M'}(0)=V_0$, $\dot{y}_{m_1}(0)=0$ – the velocity of absolutely solids at the initial time $t=t_0=0$.

$$\begin{cases} \dfrac{\partial^2 u_1(y,t)}{\partial y^2}-\dfrac{1}{a_1^2}\dfrac{\partial^2 u_1(y,t)}{\partial t^2}=0, \quad 0\le y\le l_{11}; \\ \dfrac{\partial^2 u_2(y,t)}{\partial y^2}-\dfrac{1}{a_1^2}\dfrac{\partial^2 u_2(y,t)}{\partial t^2}=0, \quad l_{11}\le y\le l_1; \\ \dfrac{\partial^2 u_3(y,t)}{\partial y^2}-\dfrac{1}{a_2^2}\dfrac{\partial^2 u_3(y,t)}{\partial t^2}=0, \quad l_1\le y\le l_1+l_{21}; \\ \dfrac{\partial^2 u_4(y,t)}{\partial y^2}-\dfrac{1}{a_2^2}\dfrac{\partial^2 u_4(y,t)}{\partial t^2}=0, \quad l_1+l_{21}\le y\le l_1+l_{20}; \\ S(y)\dfrac{\partial^2 u_5(y,t)}{\partial y^2}+\dfrac{\partial S(y)}{\partial y}\dfrac{\partial u_5(y,t)}{\partial y}-\dfrac{S(y)}{a_2}\dfrac{\partial^2 u_5(y,t)}{\partial t^2}=0, \quad l_{22}\le y\le l_2, \end{cases} \tag{9}$$

ISSN 2076-2429 (print)
ISSN 2223-3814 (online)

$$\begin{cases} \dfrac{\partial u_1(y,t)}{\partial t} = V_0, \ \dfrac{\partial u_1(y,t)}{\partial x} = 0, \quad 0 \le y \le l_{11}; \\ \dfrac{\partial u_2(y,t)}{\partial t} = V_0, \ \dfrac{\partial u_2(y,t)}{\partial x} = 0, \quad l_{11} \le y \le l_1; \\ \dfrac{\partial u_3(y,t)}{\partial t} = 0_0, \ \dfrac{\partial u_3(y,t)}{\partial x} = 0, \ l_1 \le y \le l_1 + l_{21}; \\ \dfrac{\partial u_4(y,t)}{\partial t} = 0, \quad \dfrac{\partial u_4(y,t)}{\partial x} = 0, \quad l_1 + l_{21} \le y \le l_1 + l_{20}; \\ \dfrac{\partial u_5(y,t)}{\partial t} = 0, \quad \dfrac{\partial u_5(y,t)}{\partial x} = 0, \, l_{22} \le y \le l_2; \\ y_{M'}(0) = l_{11}, \quad \dot{y}_{M'}(0) = V_0, \ y_{m_1}(0) = l_1 + l_{21}, \quad \dot{y}_{m_1}(0) = 0. \end{cases} \tag{10}$$

The boundary conditions determine the presence of forces in the section 0, as well as the conditions of the interaction of the rods in the sections X_A, X_B and absolutely solids in the sections $0'_1$, $0'_2$, X_C:

$$\begin{cases} -E_1 S_{11} \dfrac{\partial u_1(0,t)}{\partial y} = k y'_0 + c V_0, \quad \text{if} \quad \dfrac{\partial u_1(0,t)}{\partial y} < 0; \\ M' \ddot{y}_{M'} = -E_1 S_{11} \dfrac{\partial u_1(l_{11},t)}{\partial y} + E_1 S_{12} \dfrac{\partial u_2(l_{11},t)}{\partial y} + M' g - 3 p_0 S_0; \\ \dfrac{\partial u_1(l_{11},t)}{\partial t} = \dfrac{\partial u_2(l_{11},t)}{\partial t}, \quad \dot{y}_{M'} = \dfrac{\partial u_1(l_{11},t)}{\partial t}; \\ E_1 S_{12} \dfrac{\partial u_2(l_1,t)}{\partial y} - E_2 S_{12} \dfrac{\partial u_3(l_1,t)}{\partial y} = 0, \quad \text{if} \quad \dfrac{\partial u_2(l_1,t)}{\partial y} < 0; \\ \dfrac{\partial u_2(l_1,t)}{\partial t} = \dfrac{\partial u_3(l_1,t)}{\partial t}, \quad \text{if} \quad \dfrac{\partial u_2(l_1,t)}{\partial y} < 0; \\ m'_1 \ddot{y}_{m'_1} = -E_2 S_{12} \dfrac{\partial u_3(l_1 + l_{21},t)}{\partial y} + E_2 S_{22} \dfrac{\partial u_4(l_1 + l_{21},t)}{\partial y} + m'_1 g; \\ \dfrac{\partial u_3(l_1 + l_{21},t)}{\partial t} = \dfrac{\partial u_4(l_1 + l_{21},t)}{\partial y}, \quad \dot{y}_{m'_1} = \dfrac{\partial u_3(l_1 + l_{21},t)}{\partial t}; \\ \dfrac{\partial u_4(l_1 + l_{22},t)}{\partial t} = \dfrac{\partial u_5(l_1 + l_{22},t)}{\partial t}, \quad \text{if} \quad \dfrac{\partial u_1(l_1 + l_{22},t)}{\partial y} < 0; \\ E_2 S_{20} \dfrac{\partial u_5(l_1 + l_2,t)}{\partial y} - N_{67} = 0, \quad \text{if} \quad \dfrac{\partial u_5(l_1 + l_2,t)}{\partial y} < 0; \\ \dfrac{\partial u_5(l_1 + l_2,t)}{\partial t} = \dfrac{\partial u_7(l_1 + l_2,t)}{\partial t}, \quad \text{if} \quad \dfrac{\partial u_5(l_1 + l_2,t)}{\partial y} < 0. \end{cases} \tag{11}$$

We will write down the general mathematical model of the technological process of the destruction of the rock by the hinged vibro–impact device on the basis of the HPD additionally using the Navier–Stokes equation system [12], the continuity equation for the weakly liquid fluid, and also the complex of a system of stress–strain state equations for the rock 7 (Fig.3). Since the weight of the working family in relation to the total mass of the vibro impact device is insignificant, we therefore neglect the inertial forces of the working fluid itself [1, 7]. The complex of the system of equations of a stress-strain state for rock 7 will consist of: equilibrium equations [8], dependencies between displacements and deformations [9], equations of joint deformation [11] and instead of the Hooke law used in the linear theory of elasticity, to apply the system Equations in the theory of plasticity [11].

Since we have a turbulent flow regime in the hydrosystem of the vibro impact device, so in order to apply the Navier–Stokes equation system [12] we additionally use the numerical model of turbulence k–ε [10, 12].

Research results and their discussion. The mathematical model of the technological process of destruction of the rock using the vibro impact device based on the HPD, represented by systems of equations (1) – (12) and additionally by equations of hydrodynamics and stress–strain state, was implemented by numerical simulation methods based on FlowVision software systems [1], Matlab Simulink [6] and APM Structure [8] on the power of computing clusters of the Glushkov Institute of Cybernetics of National Academy of Sciences of Ukraine. The results of the simulation are the distribution of pressure in the working cavity of the HPD of the vibro impact device (Fig. 4).

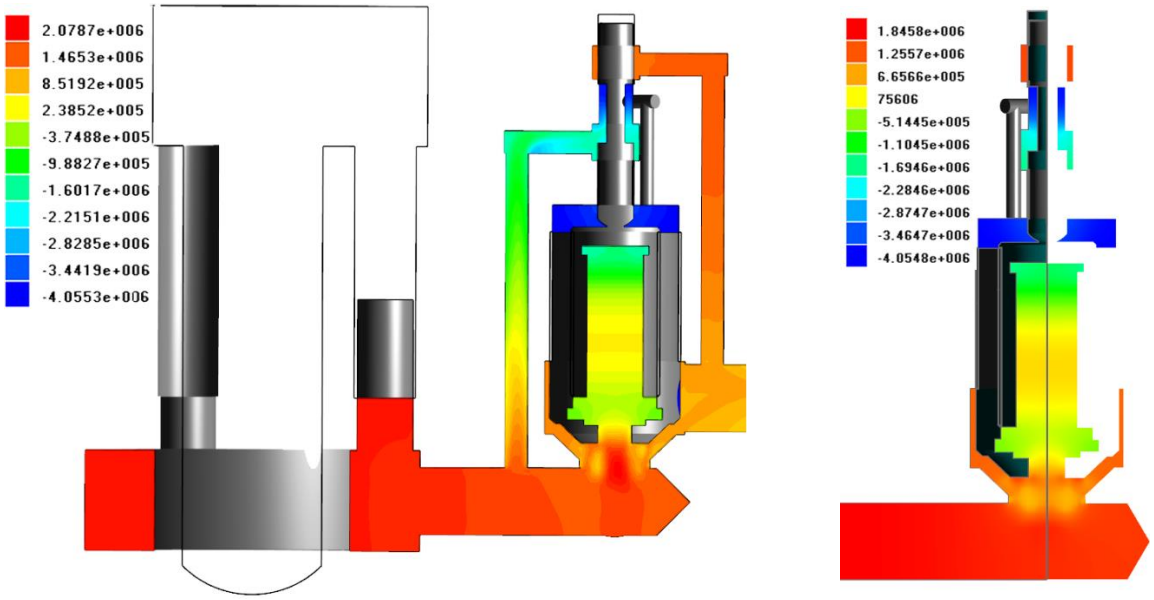

a *b*

Fig. 4. Distribution of pressure in the working cavity of the HPD of the vibro impact device: in the y0x plane (a); in the z0y plane (b)

Fig. 4 shows that in the middle cavity of the valve of the first cascade, the pressure is significantly higher than in the lower cavity. This difference in pressure creates an additional effort that allows you to move the valve of the first cascade while connecting the pressure and drain cavity.

The difference in pressure produced at the same time in the lower and upper cavities of the valve of the second cascade allows you to adjust the amplitude of the pressure in the cavity of the executive hydraulic cylinder. The use of an additional regulating cascade in the form of a valve of the first cascade can significantly reduce the size and, accordingly, the total mass of the regulating hydroequipment.

Also, one of the simulation results is the speed distribution in the working cavity of the HPD of the vibro impact device (Fig. 5).

ISSN 2076-2429 (print)
ISSN 2223-3814 (online)

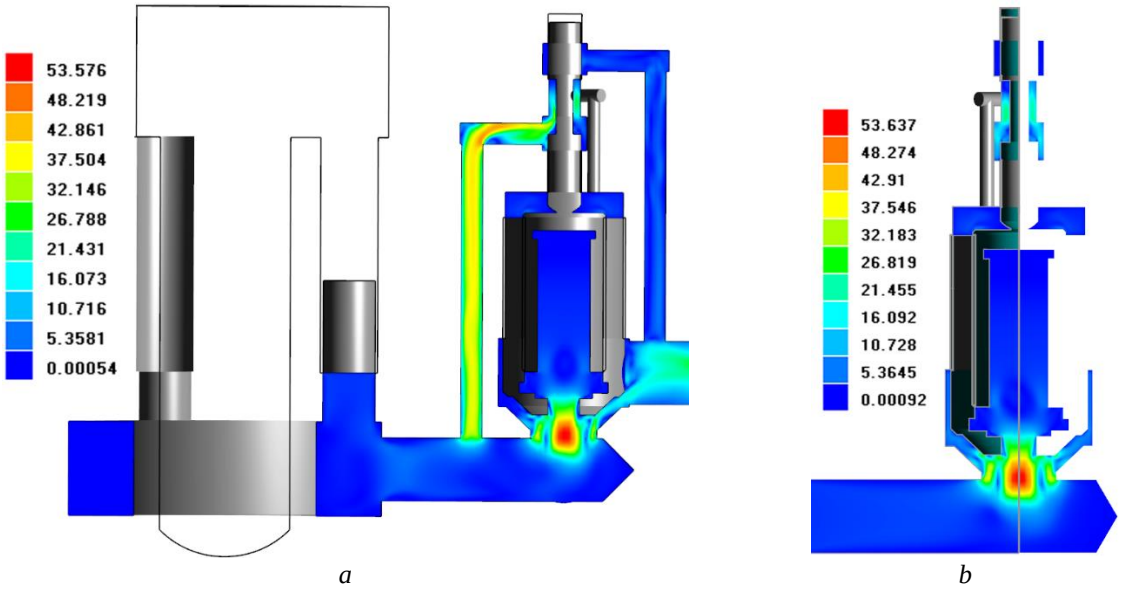

Fig. 5. Distribution of speed in the working cavity of the GIP of the vibro impact device: in the y0x plane (a); in the z0y plane (b)

Based on the results of numerical simulation (see Fig. 5, *a*), the working fluid velocity in the bottom of the valve of the second cascade is 32 m/s. This high speed of the working family forms cavitation phenomena, which negatively affects the quality of the conical surface of the valve of the second cascade. This requires the use of special material and processing mode in the manufacture of this shut–off element.

Also, the result of the calculation is a diagram of the change in pressure in the cavities of the two–stage valve–pulsator (Fig. 6).

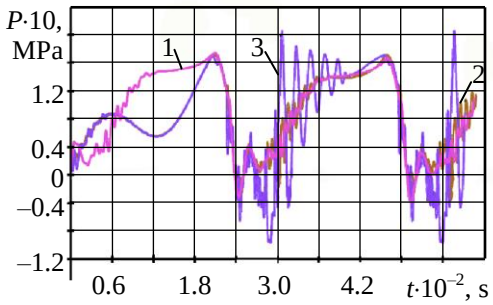

Fig. 6. Change in pressure in the working cavities of the HPD of vibro-impact device: 1 – in the cavity of the executive hydraulic cylinder; 2 – in the upper cavity of the valve of the first cascade; 3 – in the lower cavity of the valve of the first cascade

Analyzing the pressure diagrams in the corresponding cavities of the two–stage valve of the pulsator, one can conclude that the amplitude of the pressure change in the cavity of the executive cylinder is 12 MPa.

It is also possible to note that when pressure is set in the lower cavity of the valve of the first cascade there is an oscillatory pressure process that can cause an unplanned movement of the valve of the first cascade.

This phenomenon requires the construction of a valve of the first cascade so that there would be a positive overlap between the body of the HPD and the tent itself.

The next results of the calculation are the diagrams of the working parameters of the HPD (Fig. 7), namely: changes in the displacement (Fig. 7 *a*) and speed (Fig. 7 *b*) of the corresponding moving elements of the HPD.

Analyzing the diagrams (Fig. 7 *a*), moving the moving elements of the HPD can come to the conclusion:

Amplitude of oscillation of impact mass is – 10 mm; valve of the first cascade – 6 mm; the valve of the other cascade – 5 mm. The general frequency of oscillations is approximately 34 Hz.

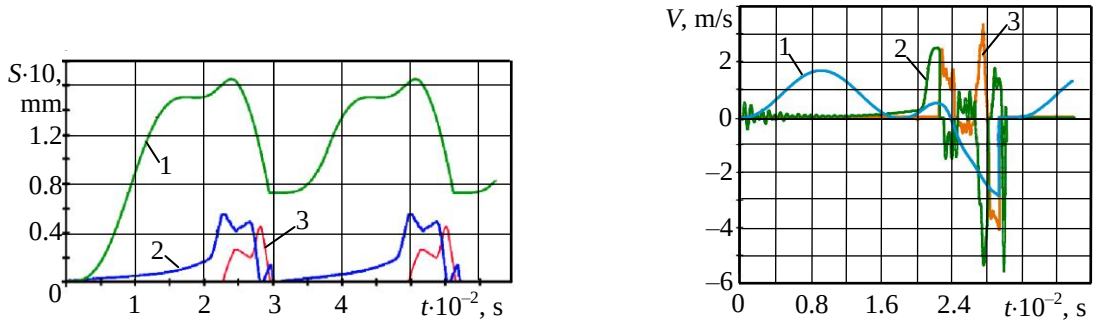

a *b*

1 – impact mass; 2 – the valve of the first cascade; 3 – the valve of the second cascade Fig. 7. Diagrams of changing the working parameters of the HPD: changes in displacement (a); change of speed (b)

Analyzing the diagrams (Fig. 7 *b*) of the velocity of moving elements of the HPD, one can come to the following conclusion.

The speed at the moment of impact of a shock mass with an executive body is 3 m/s; valve of the first cascade is 6 mm. The speed of the second stage cascade with the seating position is approximately 4 m/s, which requires a special heat treatment of the surface of the seat.

On the basis of the calculated calculations of the HPD elements using the FSI [7, 11] technology, the APM Structure program determined the stress–strain state of the executive body of the vibro impact device (Fig. 8 *a*) and the working rocks itself (Fig. 8 *b*).

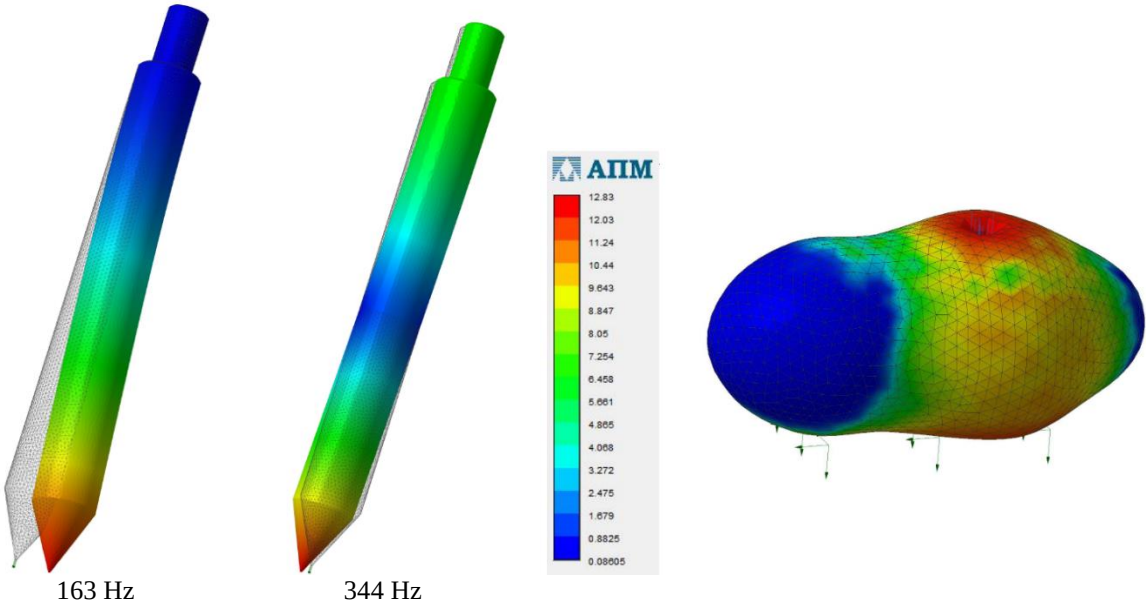

163 Hz 344 Hz

a *b*

Fig. 8. Stress–deformed state of elements of the vibro impact device: own frequency of oscillations of the executive body (a), rock (b)

ISSN 2076-2429 (print)
ISSN 2223-3814 (online)

By comparing the own oscillation frequencies of the executive body (163 Hz, 344 Hz) of the vibro impact device (see Fig. 8 *a*) and the frequency of the device itself (34 Hz), one can conclude that negative resonance phenomena are not observed. It is also possible to note the emergence of extreme stresses in the most rocky rock exposed to vibration damage.

Conclusions. An effective design of the vibro impact device based on the HPD has been developed. At the heart of the device is a two–stage valve–pulsator, to implement the most effective modes of impulse influence on the environment.

Based on the laws of hydrodynamics, using mechanorheological phenomenology and generalized mechanics laws, a new mathematical model for the study of technological processes of surface sealing of soils by inertial vibration ram is developed.

On the basis of the developed mathematical model, by means of finite volume and element methods, numerical simulations have obtained working dependences for determining the basic performance characteristics of the technological process of vibration damaging of rocks by a vibro impact device based on HPD.

The results of numerical modeling of the technological processes of vibration damaging rocks by the vibro impact device on the basis of HPD have shown the advantages of the chosen approach to design, and also allowed to prove the effectiveness of the developed design of the HPD on the basis of a two–stage valve–pulsator.

Література

1. Іскович-Лотоцький Р.Д. Технологія моделювання оцінки параметрів формоутворення заготовок з порошкових матеріалів на вібропресовому обладнанні з гідроімпульсним приводом : монографія. / Р.Д. Іскович-Лотоцький, О.В. Зелінська, Я.В. Іванчук. – Вінниця: ВНТУ, 2018. 152 с.
2. Jörg C. Response analysis of nonlinear vibro-impact system coupled with viscoelastic force under colored noise excitations / C. Jörg, K. Mont, S. Pornsak // Chemical Engineering Research and Design. 2010. Vol. 88(1). P. 100–108. DOI: 10.1016/j.cherd.2009.07.001.
3. Alessandro D. Modelling and experimental validation of a nonlinear proportional solenoid pressure control valve. International Journal of Fluid Power. Vol. 17. 2016. P. 90–101. DOI: 10.1080/14399776.2016.1141636.
4. Design and development of a test-rig for determining vibration characteristics of a beam / T. Nikhil, T. Chandrahas, C. Chaitanya, G. Sagar, R. Sabareesh // Procedia Engineering. 2016. Vol. 144. P. 312–320.
5. Eigenstructure assignment in undamped vibrating systems: a convex-constrained modification method based on receptances. / H. Ouyang, D. Richiedei, A. Trevisani, G. Zanardo // J. Sound Vibrations. No. 27. 2012. P. 397–409.
6. System-Level Coupled Modeling of Piezoelectric Vibration Energy Harvesting Systems by Joint Finite Element and Circuit Analysis / C. Cheng, Z. Chen, H. Shi, Z. Liu, Y. Xiong // Shock and Vibration. 2016. P. 1–9. DOI: 10.1155/2016/2413578.
7. Іскович-Лотоцький Р.Д. Моделювання процесу оброблення дрібнодисперсних деревинних матеріалів під дією вібраційного і віброударного навантаження / Р.Д. Іскович-Лотоцький, Я.В. Іванчук, Я.П. Веселовський // Науковий вісник НЛТУ України: збірник наукових праць. 2018. Том 28, № 5. С. 124–129. DOI: 10.15421/40280526.
8. Іванчук Я.В. Математичний метод визначення стійкості коливальних систем під дією зовнішнього вібраційного навантаження / Я.В. Іванчук // Технічні науки та технології. 2018. № 2 (12). С. 25–33 . DOI: 10.25140/2411-5363-2018-2(12)-25-33.
9. Яровий А.А. Методи та засоби організації високопродуктивних паралельно-ієрархічних обчислювальних систем із рекурсивною архітектурою : монографія / А.А. Яровий/ Вінниця: ВНТУ, 2016. 363 с.
10. Wilcox D.C. Turbulence modeling for CFD / D.C. Wilcox. – DCW Industries, Inc., 1994. 460 p.
11. New approach for the detection of noise-distorted signals based on the method of S-preparation / L.I. Timchenko, Yu.F. Kutayev, S.V. Cheporniuk, N.I. Kokriatskaya, A.A. Yarovyy, A.E. Denysova // IET Image Processing. 2014. Vol. 8, Issue 11. P. 627–638. DOI: 10.1049/iet-ipr.2013.0471.

12. Abolfathia A. Investigating the sources of variability in the dynamic response of built-up structures through a linear analytical model / A. Abolfathia, D.J. O'Boy, S.J. Walsha, S.A. Fisherb // Journal of Sound and Vibration. 2017. Vol. 387. P. 163–176.

References

1. Iskovych-Lototsky, R. D., Zelinska, O. V., & Ivanchuk, Y. V. (2018). *The technology of modeling the evaluation of the parameters of forming blanks of powder materials on the vibropress equipment with a hydro-pulse drive.* Monograph. Vinnytsia: VNTU.
2. Jörg, C., Mont, K., & Pornsak, S. (2010). Response analysis of nonlinear vibro-impact system coupled with viscoelastic force under colored noise excitations. *Chemical Engineering Research and Design, 88(1),* 100–108. DOI: 10.1016/j.cherd.2009.07.001.
3. Alessandro, D. (2016). Modelling and experimental validation of a nonlinear proportional solenoid pressure control valve. *International Journal of Fluid Power, 17,* 90–101. DOI: 10.1080/14399776.2016.1141636.
4. Nikhil, T., Chandrahas, T., Chaitanya, C., Sagar, G., & Sabareesh, R. (2016). Design and development of a test-rig for determining vibration characteristics of a beam. *Procedia Engineering, 144*, 312–320.
5. Ouyang, H., Richiedei, D., Trevisani, A. & Zanardo, G. (2012). Eigenstructure assignment in undamped vibrating systems: a convex-constrained modification method based on receptances. *J. Sound Vibrations, 27*, 397–409.
6. Cheng, C., Chen, Z., Shi, H., Liu, Z., & Xiong, Y. (2016). System-Level Coupled Modeling of Piezoelectric Vibration Energy Harvesting Systems by Joint Finite Element and Circuit Analysis. *Shock and Vibration*, 1–9. DOI: 10.1155/2016/2413578.
7. Iskovych-Lototsky, R. D., Ivanchuk, Y. V., & Veselovsky, Y. P. (2018). Modeling the processing of fine wood materials under the action of vibration and vibro-impact load. *Scientific Bulletin of UNFU, 28, 5,* 124–129. DOI: 10.15421/40280526.
8. Ivanchuk, Y. V. (2018). Mathematical method for determining the stability of oscillatory systems under the action of external vibrations. *Technical sciences and technologies, 2 (12)*, 25–33. DOI: 10.25140/2411-5363-2018-2(12)-25-33.
9. Yarovui, A. A. (2016). *Methods and means of organizing high-performance parallel-hierarchical computing systems with recursive architecture*. Monograph. Vinnytsia: VNTU.
10. Wilcox, D. C. (1994). *Turbulence modeling for CFD*. DCW Industries, Inc.
11. Timchenko, L. I., Kutayev, Yu. F., Cheporniuk, S. V., Kokriatskaya, N. I., Yarovyy, A. A., & Denysova, A. E. (2014). New approach for the detection of noise-distorted signals based on the method of S-preparation. *IET Image Processing, 8, 11*, 627–638. DOI: 10.1049/iet-ipr.2013.0471.
12. Abolfathia, A., O'Boy, D. J., Walsha, S. J., & Fisherb, S. A. (2017). Investigating the sources of variability in the dynamic response of built-up structures through a linear analytical model. *Journal of Sound and Vibration, 387,* 163–176.

Іванчук Ярослав Володимирович; Ivanchuk Yaroslav, ORCID: http:// orcid.org/ 0000-0002-4775-6505